ELSEVIER

Physica D 96 (1996) 47–65

PHYSICA D

Numerical study of a Lyapunov functional for the complex Ginzburg–Landau equation

R. Montagne *,[1], E. Hernández-García [2], M. San Miguel [3]

Departament de Física, Universitat de les Illes Balears, and Institut Mediterrani d'Estudis Avançats, IMEDEA (CSIC-UIB), E-07071 Palma de Mallorca, Spain

Abstract

We numerically study in the one-dimensional case the validity of the functional calculated by Graham and coworkers (Graham and Tel, 1990; Descalzi and Graham, 1994) as a Lyapunov potential for the Complex Ginzburg–Landau equation. In non-chaotic regions of parameter space the functional decreases monotonically in time towards the plane wave attractors, as expected for a Lyapunov functional, provided that no phase singularities are encountered. In the phase turbulence region the potential relaxes towards a value characteristic of the phase turbulent attractor, and the dynamics there approximately preserves a constant value. However, there are very small but systematic deviations from the theoretical predictions, that increase when going deeper in the phase turbulence region. In more disordered chaotic regimes characterized by the presence of phase singularities the functional is ill-defined and then not a correct Lyapunov potential.

PACS: 05.45.+b; 05.70.Ln

Keywords: Complex Ginzburg–Landau equation; Non-equilibrium potential; Lyapunov potential; Spatio-temporal chaos

1. Introduction

The Complex Ginzburg–Landau Equation (CGLE) is the amplitude equation describing universal features of the dynamics of extended systems near a Hopf bifurcation [1,2].

$$\partial_t A = aA + (D_r + \mathrm{i}D_i)\nabla^2 A - (b_r + \mathrm{i}b_i) \mid A \mid^2 A. \tag{1.1}$$

Examples of this situation include binary fluid convection [3], transversally extended lasers [4] and chemical turbulence [5]. We will consider here only the one-dimensional case, $A = A(x, t)$, with $x \in [0, L]$. Suitable scaling of the complex amplitude A, space, and time shows that for fixed sign of a there are only three independent parameters in (1.1) (with D_r and $b_r > 0$ that we assume henceforth). They can be chosen to be L, $c_1 \equiv D_i/D_r$, and $c_2 \equiv b_i/b_r$.

The CGLE for $a > 0$ displays a rich variety of complex spatio-temporal dynamical regimes that have been recently classified in a phase diagram in the parameter space $\{c_1, c_2\}$ [6–8]. It is commonly stated that such non-trivial dynamical behavior, occurring also in other non-equilibrium systems, originates from the non-potential or non-variational character of the dynamics [9]. This general statement needs to be qualified because it involves some confusion in the

* Corresponding author. E-mail: montagne@hp1.uib.es.

[1] on leave from Universidad de la República (Uruguay).

[2] E-mail: dfsehg4@ps.uib.es.

[3] E-mail: dfsmsm0@ps.uib.es.

PII S0167-2789(96)00013-9

terminology. For example the term "non-variational" is often used meaning that there is no Lyapunov functional for the dynamics. But Graham and coworkers, in a series of papers [10–14], have shown that a Lyapunov functional does exist for the CGLE, and they have constructed it approximately in a small-gradient approximation. The correct statement for the CGLE is that it is not a gradient flow. This means that there is no real functional of A from which the right-hand side of (1.1) could be obtained by functional derivation.

Part of the confusion associated with the qualification of "non-variational" dynamics comes from the idea that the dynamics of systems having non-trivial attractors, such as limit cycles or strange chaotic attractors, cannot be deduced from the minimization of a potential which plays the role of the free energy of equilibrium systems. However, such idea does not preclude the existence of a Lyapunov functional for the dynamics. The Lyapunov functional can have local minima which identify the attractors. Once the system has reached an attractor which is not a fixed point, dynamics can proceed on the attractor due to "non-variational" contributions to the dynamical flow which do not change the value of the Lyapunov functional. This just means that the dynamical flow is not entirely determined once the Lyapunov functional is known. This situation is very common and well known in the study of dynamical properties within the framework of conventional statistical mechanics: The equilibrium free energy of the system is a Lyapunov functional for the dynamics, but equilibrium critical dynamics [15] usually involves contributions, such as mode–mode coupling terms, which are not determined just by the free energy. The fact that the dynamical evolution is not simply given by the minimization of the free energy is also true when studying the non-equilibrium dynamics of a phase transition in which the system evolves between an initial and a final equilibrium state after, for example, a jump in temperature across the critical point [16].

A Lyapunov functional plays the role of a potential which is useful in characterizing global properties of the dynamics, such as attractors, relative or nonlinear stability of these attractors, etc. In fact, finding such potentials is one of the long-sought goals of non-equilibrium physics [17,18], the hope being that they should be instrumental in the characterization of non-equilibrium phenomena through phase transition analogies. The use of powerful and very general methods based on these analogies has been advocated by a number of authors [6–8,19,20]. In this context, it is a little surprising that the finding of a Lyapunov functional for the CGLE [12–14] has not received much attention in the literature. A possible reason for this is that the construction of non-equilibrium potentials has been historically associated with the study of stochastic processes, in particular in the search of stationary probability distributions for systems driven by random noise [17,18,21]. We want to make clear that the finding of the Lyapunov functional for the CGLE [12–14] as well as the whole approach and discussion in the present paper is completely within a purely deterministic framework and it does not rely on any noise considerations. A second possible reason for the relative little attention paid to the Lyapunov functional for the CGLE is the lack of any numerical check of the uncontrolled approximations made on its derivation. The main purpose of this paper is precisely to report such numerical check of the results of Graham and collaborators, thus delimiting the range of validity of the approximations involved. We also provide a characterization of the time evolution of the Lyapunov functional in different regions of the phase diagram of the CGLE [6–8], which illustrates the use of such potential.

Our main findings are that the expressions by Graham and coworkers behave to a good approximation as a proper Lyapunov potential when phase singularities (vanishing of the modulus of A) are not present. This includes non-chaotic regimes as well as states of phase turbulence. In this last case some small but systematic discrepancies with the predictions are found. In the presence of phase singularities the potential is ill-defined and then it is not a correct Lyapunov functional.

The paper is organized as follows. For pedagogical purposes, we first discuss in Section 2 a classification of dynamical flows in which notions like relaxational or potential flows are considered. The idea of a potential for the CGLE is clearer in this context.

In Section 3 we review basic phenomenology of the CGLE and the main analytical results for the Lyapunov functional of the CGLE. Sections 4 and 5 contain our numerical analyses. Section 4 is devoted to the Benjamin–Feir stable regime of the CGLE and Section 5 to the phase turbulent regime. Our main conclusions are summarized in Section 6.

2. A classification of dynamical flows

In the following we review a classification of dynamical systems that, although rather well established in other contexts [17,18], it is often overlooked in general discussions of deterministic spatio-temporal dynamics. Non-potential dynamical systems are often defined as those for which there is no Lyapunov potential. Unfortunately, this definition is also applied to cases in which there is no *known* Lyapunov potential. To be more precise, let us consider dynamical systems of the general form

$$\partial_t A_i = V_i[A], \tag{2.1}$$

where A_i represents a set of, generally complex, dynamical variables which are spatially dependent fields: $A_i = A_i(\mathbf{x}, t)$. $V_i[A]$ is a functional of them. The notation A_i^* represents the complex conjugate of A_i and for simplicity we will keep the index i implicit. Let us now split V into two contributions:

$$V[A] = G[A] + N[A] , \tag{2.2}$$

where G, the *relaxational* part, will have the form

$$G[A] = -\frac{\Gamma}{2}\frac{\delta F[A]}{\delta A^*} \tag{2.3}$$

with F a real and scalar functional of A. Γ is an arbitrary hermitic and positive-definite operator (possibly depending on A). In the particular case of real variables there is no need of taking the complex conjugate, and hermitic operators reduce to symmetric ones. The functional $N[A]$ in (2.2) is the remaining part of $V[A]$. The important point is that, if the splitting (2.2) can be done in such a way that the following orthogonality condition is satisfied (c.c. denotes the complex conjugate expression):

$$\int \mathrm{d}\mathbf{x}\left(\frac{\delta F[A]}{\delta A(\mathbf{x})}N[A(\mathbf{x})] + \text{c.c.}\right) = 0 , \tag{2.4}$$

then the terms in N neither increase nor decrease the value of F, which due to the terms in G becomes a decreasing function of time:

$$\frac{\mathrm{d}F[A(\mathbf{x}, t)]}{\mathrm{d}t} \leq 0 . \tag{2.5}$$

If F is bounded from below then it is a Lyapunov potential for the dynamics (2.1). Eq. (2.6) with $N = V - G$, that is

$$\int \mathrm{d}\mathbf{x}\left(\frac{\delta F[A]}{\delta A(\mathbf{x})}\left(V[A(\mathbf{x})] + \frac{\Gamma}{2}\frac{\delta F[A]}{\delta A^*(\mathbf{x})}\right) + \text{c.c.}\right) = 0, \tag{2.6}$$

can be interpreted as an equation for the Lyapunov potential F associated to a given dynamical system (2.1). It has a Hamilton–Jacobi structure. When dealing with systems perturbed by random noise, Γ is fixed by statistical requirements, but in deterministic contexts such as the present paper, it can be arbitrarily chosen in order to simplify (2.6).

Solving (2.6) is in general a difficult task, but a number of non-trivial examples of the splitting (2.2)–(2.5) exist in the literature. Some of these examples correspond to solutions of (2.6) found in the search of potentials for dynamical systems [10–12]. Other examples just correspond to a natural splitting of dissipative and non-dissipative contributions in the dynamics of systems with well established equilibrium thermodynamics, as for example models of critical dynamics [15] or the equations of nematodynamics in liquid crystals [22].

Once the notation above has been set up, we can call relaxational systems those for which there is a solution F of (2.6) such that $N = 0$, that is all the terms in V contribute to decrease F. Potential systems can be defined as those for which there is a non-trivial (i.e. a non-constant) solution F to (2.6). In relaxational systems there is no long-time dynamics, since there is no time evolution of A once a minimum of F is reached. On the contrary, for potential systems for which $N \neq 0$, the minima of F define the attractors of the dynamical flow, but once one of these attractors is reached, non-trivial sustained dynamics might exist

on the attractor. Such dynamics is determined by N and maintains a constant value for the functional F.

A possible more detailed classification of the dynamical flows is the following:

(1) *Relaxational gradient flows*: Those dynamical systems for which $N = 0$ with Γ proportional to the identity operator. In this case the time evolution of the system follows the lines of steepest descent of F. A well-known example is the so-called Fisher–Kolmogorov equation, also known as model A of critical dynamics [15], or (real) Ginzburg–Landau equation for a real field $A(\mathbf{x}, t)$

$$\dot{A} = \alpha A + \gamma \nabla^2 A - \beta \mid A \mid^2 A \,, \tag{2.7}$$

where α, γ and β are real coefficients. This equation is of the form of Eqs. (2.1)–(2.3) with $N = 0$, $\Gamma = 1$, and $F = F_{\mathrm{GL}}[A]$, the Ginzburg–Landau free energy:

$$F_{\mathrm{GL}}[A] = \int \mathrm{d}\mathbf{x} \left(-\alpha \mid A \mid^2 + \gamma \mid \nabla A \mid^2 + \frac{\beta}{2} \mid A \mid^4 \right). \tag{2.8}$$

(2) *Relaxational non-gradient flows*: Still $N = 0$ but with Γ not proportional to the identity, so that the relaxation to the minimum of F does not follow the lines of steepest descent of F. The matrix operator Γ might depend on A or involve spatial derivatives. A well-known example of this type is the Cahn–Hilliard equation of spinodal decomposition, or model B of critical dynamics for a real variable A. [15]:

$$\dot{A} = \left(-\frac{1}{2} \nabla^2 \right) \left(-\frac{\delta F_{\mathrm{GL}}[A]}{\delta A} \right). \tag{2.9}$$

The symmetric and positive-definite operator $(-\nabla^2)$ has its origin in a conservation law for A.

(3) *Non-relaxational potential flows*: N does not vanish, but the potential F, solution of (2.6) exists and is non-trivial. Most models used in equilibrium critical dynamics [15] include non-relaxational contributions, and therefore belong to this category. A particularly simple example is

$$\dot{A} = -(1 + \mathrm{i}) \frac{\delta F_{\mathrm{GL}}[A]}{\delta A^*}, \tag{2.10}$$

where now A is a complex field. Notice that we can not interpret this equation as being of type 1, because $(1 + \mathrm{i})$ is not a hermitic operator, but still F_{GL} is a Lyapunov functional for the dynamics. Eq. (2.10) is a special case of the CGLE, in which $V[A]$ is the sum of a relaxational gradient flow and a non-linear-Schrödinger-type term $N[A] = -i(\delta F_{\mathrm{GL}}[A]/\delta A^*)$.

The general CGLE [2] is of the form (2.7) but A is complex and α, γ and β are arbitrary complex numbers. For the special case in which $\mathrm{Re}[\Gamma]/\mathrm{Im}[\Gamma] = \mathrm{Re}[\beta]/\mathrm{Im}[\beta]$, as for example in (2.10), the Lyapunov functional for the CGLE is known exactly [23]. Such choice of parameters has important dynamical consequences [24]. Beyond such special cases, the calculations by Graham and coworkers indicate [13,14] that the CGLE, a paradigm of complex spatio-temporal dynamics, might be classified within this class of non-relaxational potential flows because a solution of (2.6) is found. The difficulty is that the explicit form of the potential is, so far, only known as an uncontrolled small-gradient expansion.

(4) *Non-potential flows*: Those for which the only solutions F of (2.6) are the trivial ones (that is $F =$ constant). Hamiltonian systems as for example the non-linear Schrödinger equation are of this type.

3. A Lyapunov functional for the CGLE

It is well known that for $a < 0$ the one-dimensional CGLE (1.1) has $A = 0$ as a stable solution, whereas for $a > 0$ there are Travelling Wave (TW) solutions of the form

$$A_k = A_0 \mathrm{e}^{\mathrm{i}(kx + \omega t) + \varphi_0} \tag{3.1}$$

with $A_0 = \sqrt{(a - D_r k^2)/b_r}$, $|k| < \sqrt{a/b_r}$, and $\omega = (b_i a + D_- k^2)/b_r$. We have introduced

$$D_- \equiv D_r b_i - D_i b_r \,. \tag{3.2}$$

φ_0 is any arbitrary constant phase.

The linear stability of the homogeneous solution ((3.1) with $k = 0$) with respect to long wavelength fluctuations divides the parameter space $\{c_1, c_2\}$ in two

regions: the Benjamin–Feir (BF) stable and the BF unstable zone. This line is given by [25,26]

$$D_+ \equiv D_r b_r + D_i b_i = 0. \tag{3.3}$$

In the BF unstable region ($D_+ < 0$) there are no stable TW solutions, while in the BF stable region ($D_+ > 0$) TW's with a wave number $k < k_E$ are linearly stable. For $k > k_E$, TW's become unstable through the long wavelength instability known as the Eckhaus instability [27,28]. The Eckhaus wave number k_E is given by

$$k_E^2 = \frac{a b_r D_+}{D_r(3D_+ b_r + 2D_- b_i)}. \tag{3.4}$$

Recent numerical work for $a > 0$ and L large [6–8,29] has identified regions of the parameter space displaying different kinds of regular and spatio-temporal chaotic behavior (obtained at long times from random initial conditions and periodic boundary conditions), leading to a "phase diagram" for the CGLE. The five different regions, each leading to a different asymptotic phase, are shown in Fig. 1 as a function of the parameters c_1 and c_2 ($a > 0$, L large). Two of these regions are in the BF stable zone and the other three in the BF unstable one. One of the main distinctions between the different asymptotic phases is in the behavior of the modulus of A at long times. In some regions it never vanishes, whereas in others it vanishes from time to time at different points. A more detailed description of the asymptotic behavior in the different regions is as follows:

(i) *Non-chaotic region.* The evolution here ends in one of the Eckhaus-stable TW solutions for almost all the initial conditions.

(ii) *Spatio-temporal intermittency region.* Despite the fact that there exist stable TW, the evolution from random initial conditions is not attracted by them but by a chaotic attractor in which typical configurations of the field A consist of patches of TW interrupted by turbulent bursts. The modulus of A in such bursts typically touches zero quite often.

(iii) *Defect turbulence.* This is a strongly disordered phase in which the modulus of A has a finite density of space–time zeros. In addition the space and time correlation functions have a quasi-exponential decay [6,7].

(iv) *Phase turbulence.* This is a weakly disordered phase in which $|A(x, t)|$ remains away from zero. The temporal correlations decay slower than exponentially [6,7].

(v) *Bi-chaos region.* Depending on the particular initial condition, the system ends on attractors similar to the ones in regions 3, 4, or in a new attractor in which the configurations of A consist of patches of phase and defect turbulence.

An approximate Lyapunov functional for the CGLE was calculated by Graham and collaborators [13,14,30]. Earlier attempts to find a Lyapunov functional were based on polynomial expansions [23,31–33], while more recent and successful approaches focused in solving the Hamilton–Jacobi equation (2.6) with $\Gamma = 1$ in different ways. This was done first by a minimization procedure involving an action integral [10–12], and more recently by a more direct expansion method [13,14,30]. This last method provides also expressions in higher dimensions, but we will restrict here to the one-dimensional case. In any case, the solution involves an uncontrolled gradient expansion around space-independent solutions of the CGLE. Such expansion obviously limits the validity of the result to regions in the phase diagram in which there are not strong gradients. This excludes the regions in which zeros in the modulus of A are typical, since the phase of A becomes singular there. In particular spatio-temporal intermittency regimes, bi-chaos and defect turbulence are out of the range of validity of Graham's expansion. The meaningfulness of the potential in the other regions of parameter space remains still an open question because of the uncontrolled small gradient approximations used to calculate it, and calls for some numerical check.

In their solution of the Hamilton–Jacobi equation, Graham and collaborators find different branches of the Lyapunov functional with expressions valid for different values of the parameters. In particular they identify the BF line (3.3) as separating two branches of the solution to (2.6).

The explicit expressions (obtained with $\Gamma = 1$) are given in polar coordinates:

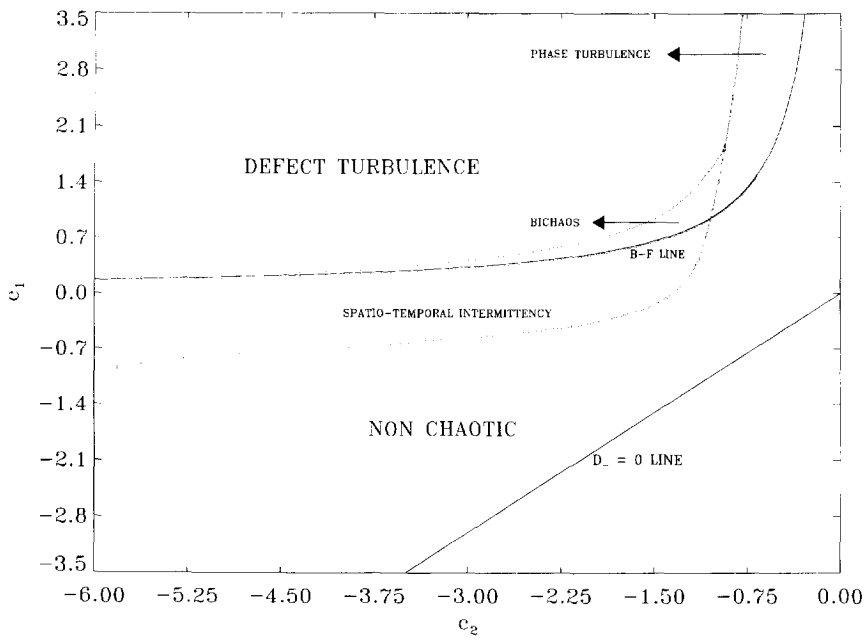

Fig. 1. Regions of the parameter $[c_1 - c_2]$-space ($a = 1$) for the $d = 1$ CGLE displaying different kinds of regular and chaotic behavior. Two analytically obtained lines, the Benjamin–Feir line (B–F line) and the D_- line, are also shown.

$$A(x,t) = r(x,t)e^{i\varphi(x,t)}. \tag{3.5}$$

In terms of the amplitude r, the phase φ, and their spatial derivates (denoted as r_x, φ_x,φ_{xx}, etc.) the Lyapunov functional per unit of length $\Phi \equiv F/L$ was found [13,14] for $a < 0$:

$$\Phi = \int \left\{ b_r r^4 - 2ar^2 + 2\left[D_r + \frac{D_- b_i r^4}{3(a - b_r r^2)^2} \right] r_x^2 - \frac{2D_- r^3}{3(a - b_r r^2)} r_x \varphi_x + 2D_r r^2 \varphi_x^2 \right\} dx. \tag{3.6}$$

We note that even in this relatively simple case $a < 0$, the result for Φ is only approximate and its structure reveals a highly non-trivial dynamics.

For $a > 0$, in the BF stable region ($D_+ > 0$) the expression for Φ results:

$$\begin{aligned}\Phi = \int \Bigg\{ & b_r r^4 - 2ar^2 + \Big[(A_1 r + B_1/r^2) r_x^2 \\ & + (A_2 r + B_2/r) r_x \varphi_x \\ & + 2(D_r r^2 - D_- b_i a/ \mid b \mid^2 b_r) \varphi_x^2 \Big] \\ & + \Big[\frac{D_- D_r b_i}{3 b_r \mid b \mid^2} \varphi_x^4 \\ & + \Big(- \frac{D_-^2 a}{2 b_r^4 r^2} \\ & - \frac{D_-}{b_r^2} (D_-/b_r + 2D_i) \ln r + C_1 \Big) \varphi_{xx}^2 \\ & + \frac{2D_- D_r}{3 b_r^2 \mid b \mid^2} (b_i^2 - b_r^2) \frac{\varphi_x^3 r_x}{r} \\ & + \frac{2D_- D_r b_i}{3 b_r^3 \mid b \mid^2} (b_i^2 - 2b_r^2) \frac{\varphi_x^2 r_x^2}{r^2} \\ & - \frac{4 D_r b_i D_-}{3 b_r^3 r} \left(1 + \frac{\ln(b_r r^2/a)}{1 - b_r r^2/a} \right) r_x \varphi_x \varphi_{xx} \Big] \Bigg\} dx, \end{aligned} \tag{3.7}$$

where:

$$\begin{aligned} A_1 &= 2(D_r + b_i D_-/3b_r^2), \\ A_2 &= 2D_-/b_r, \\ B_1 &= \frac{2D_- b_i a}{3 b_r^3 \mid b \mid^2} (2b_r^2 - b_i^2), \\ B_2 &= \frac{2D_- a}{b_r^2 \mid b \mid^2} (b_r^2 - b_i^2). \end{aligned} \tag{3.8}$$

Clearly, Φ is ill-defined when $r = 0$.

By writing-out the Euler–Lagrange equations associated to the minimization of Φ the TW solutions (3.1) are identified as local extrema of Φ. Since they occur in families parametrized by the arbitrary phase φ_0, the minima associated to the TW of a given k are not isolated points but lay on a one-dimensional closed manifold. The non-variational part of the dynamics (N in (2.2)) can be explicitly written-down by subtracting $G = -(1/2)(\delta F/\delta A^*)$ with $F = L\Phi$ to the right-hand-side of (1.1). It is seen to produce, when evaluated on the manifold of minima of Φ with a given k, constant motion along it. This produces the periodic time dependence in (3.1) and identifies the TW attractors as limit cycles.

The value of k for which the corresponding extrema change character from local minima to saddle points is precisely the Eckhaus wave number k_E. It is remarkable that, although expression (3.7) was obtained in a gradient expansion around the homogeneous TW, their minima identify exactly all the TW's of Eq. (1.1), and their frequencies and points of instability are also exactly reproduced. This gives confidence on the validity of Graham's approximations. However, it should be stressed that they are not exact and can lead to unphysical consequences. For instance, the value of the potential Φ evaluated on a TW of wave-number k ($|k| < \sqrt{a/b_r}$) is [12]

$$\Phi_k \equiv \Phi[A_k] = \frac{2D_+ a}{|b|^2}k^2\left(1 - \frac{k^2}{6k_E^2}\right) + \Phi_{k=0}, \tag{3.9}$$

where $\Phi_{k=0} = -a^2/b_r$. For a range of parameter values this expression gives mathematical sense to the intuitive fact that the closer to zero k is the more stable is the associated TW (because its potential is lower). But for some parameter values the minimal potential corresponds to large wave numbers close to $\pm\sqrt{a/b_r}$. This is counterintuitive and calls for some numerical test. The test will be described below and it will be shown that the wave numbers close to $\pm\sqrt{a/b_r}$ are out of the range of validity of the small gradient approximations leading to (3.7).

We already mentioned in Section 2 that the Lyapunov functional for the CGLE is exactly known for special values of the parameters [12,13,24]. This happens for $D_- \equiv D_r b_i - D_i b_r = 0$, which lies in the BF-stable region as indicated in Fig. 1 . In this case it is clear that (1.1) can be written as

$$\dot{A} = -\frac{1}{2}\frac{\delta F_{GL}[A]}{\delta A^*} + ib_i\left(-|A|^2 + \frac{D_r}{b_r}\nabla^2\right)A, \tag{3.10}$$

where $F_{GL}[A]$ is (2.8) for complex A and with $\alpha = 2a$, $\beta = 2b_r$, and $\gamma = 2D_r$. It is readily shown that the term proportional to b_i is orthogonal to the gradient part, so that F_{GL} is an exact solution of (2.6) for these values of the parameters, and (3.10) is a relaxational non-gradient flow (see classification in Section 2). It is seen that the approximate expressions (3.6) and (3.7) greatly simplify when $D_- = 0$ leading both to the same expression:

$$L\Phi = \int\left\{-2ar^2 + b_r r^4 + 2D_r r r_x^2 + 2D_r r^2\varphi_x^2\right\}\mathrm{d}x. \tag{3.11}$$

When expressed in terms of A and A^* it reproduces F_{GL} in (3.10). Thus the gradient expansion turns out to be exact on the line $D_- = 0$.

In the Benjamin–Feir unstable region ($a > 0$, $D_+ < 0$) the gradient expansion for Φ becomes [14, 30]:

$$\begin{aligned}\Phi = \int\Bigg\{ & b_r r^4 - 2ar^2 + \Bigg[(A_1 r + \tilde{B}_1/r^2)r_x^2 \\ & + (A_2 r + \tilde{B}_2/r)r_x\varphi_x + 2D_r\left(r^2 - \frac{a}{b_r}\right)\varphi_x^2\Bigg] \\ & + \Bigg[\frac{D_r^2}{b_r}\varphi_x^4 + \Bigg(\frac{b_r}{2a^2r^2}\Bigg(\frac{\tilde{B}_2^2}{4} \\ & + \frac{4D_r^2a^2}{b_r^2}\Bigg)\left(r^2 - \frac{a}{b_r}\right) \\ & - \frac{A_2}{2b_r}\left(\frac{A_2}{4} + D_i\right)\ln\left(\frac{r^2 b_r}{a}\right) + \frac{D_i^2}{b_r}\Bigg)\varphi_{xx}^2 \\ & - \frac{4D_r b_i D_-}{b_r^3 r}\Bigg(1 + \frac{D_r|b|^2 + 2b_r D_+}{b_i D_-\left(1 - \frac{b_r r^2}{a}\right)} \\ & \times \ln\left(\frac{r^2 b_r}{a}\right)\Bigg)\varphi_x r_x \varphi_{xx}\end{aligned}$$

$$+\frac{2D_r}{3b_r^2 r}(5b_iD_r + D_ib_r)\varphi_x^3 r_x + \frac{2b_iD_r}{3b_r^3 r^2}(7b_iD_r + D_ib_r)\varphi_x^2 r_x^2\Big]\Big\}\,\mathrm{d}x, \tag{3.12}$$

where in addition to the previous definitions

$$\tilde{B}_1 = -\frac{2ab_i}{3b_r^3}(D_rb_i + 2D_ib_r),$$
$$\tilde{B}_2 = -\frac{2a}{b_r^2}(D_rb_i + D_ib_r). \tag{3.13}$$

It was noted before that this expression can be adequate, at most, for the phase turbulent regime, since in the other BF unstable regimes $|A|$ vanishes at some points and instants, so that (3.12) is ill-defined.

The long time dynamics occurs in the attractor defined by the minima of Φ. The Euler–Lagrange equations associated to the minimization of (3.12) lead to a relationship between amplitude and phase of A which implies the well-known adiabatic following of the amplitude to the phase dynamics commonly used to describe the phase turbulence regime by a non-linear phase equation. The explicit form of this relationship is

$$r^2 = \frac{a}{br} - \frac{D_r}{b_r}(\nabla\varphi)^2 - \frac{D_i}{b_r}\nabla^2\varphi + \frac{b_iD_i^2}{2ab_r^2}\nabla^4\varphi + 2\frac{D_rD_ib_i}{ab_r^2}\nabla\varphi\nabla^3\varphi + 2\frac{b_iD_r^2}{ab_r^2}\nabla\varphi\nabla\nabla^2\varphi + \left[\frac{D_rD_ib_i}{ab_r^2} - \frac{|D|^2}{ab_r}\right](\nabla^2\varphi)^2. \tag{3.14}$$

It defines the attractor characterizing the phase turbulent regime. Dynamics in this attractor follows from the non-relaxational part N in (2.2). When (3.14) is imposed in such non-relaxational part of the dynamics the generalized Kuramoto–Shivashinsky equation containing terms up to fourth order in the gradients [34] is obtained [14,30].

We finally note that in the phase turbulent regime the Lyapunov functional Φ gives the same value [14,30] when evaluated for any configuration satisfying (3.14), at least within the small gradient approximation. This corresponds to the evolution on a chaotic attractor (associated to the Kuramoto–Sivashinsky dynamics coming from N) which is itself embedded in a region of constant Φ (the potential plateau [18]). This plateau consists of the functional minima of Φ (3.14). All the (unstable) TW are also contained in the same plateau, since they satisfy (3.14).

4. Numerical studies of the Lyapunov functional in the Benjamin–Feir stable regime

We numerically investigate the validity of $\Phi[A]$ in (3.6), (3.7), and (3.12) as an approximate Lyapunov functional for the CGLE. When evaluated on solutions $A(x,t)$ of (1.1) it should behave as a monotonously decreasing function of time, until $A(x,t)$ reaches the asymptotic attractor. After then, Φ should maintain in time a constant value characteristic of the particular attractor.

All the results reported here were obtained using a pseudo-spectral code with periodic boundary conditions and second-order accuracy in time. Spatial resolution was typically 512 modes, with runs of up to 4096 modes to confirm the results. Time step was typically $\Delta t = 0.1$ except when differently stated in the figure captions. Since very small effects have been explored, care has been taken of confirming the invariance of the results with decreasing time step and increasing number of modes. System size was always taken as $L = 512$, and always $D_r = 1$ and $b_i = -1$, so that $c_1 = D_i$ and $c_2 = -1/b_r$. When a random noise of amplitude ϵ is said to be used as or added to an initial condition it means that a set of uncorrelated Gaussian numbers of zero mean and variance ϵ^2 was generated, one for each collocation point in the numerical lattice.

4.1. Negative a

The uniform state $A = 0$ is stable for $a < 0$. We start our numerical simulation with a plane wave $A = A_0 e^{ikx}$ of arbitrary wave number $k = 0.295$ and arbitrary amplitude $A_0 = 1$ (note that the TW's (3.1) do not exist for $a < 0$), and calculate Φ for the evolving configurations. In order to have relevant non-linear effects during the relaxation towards $A = 0$ we have

chosen a small value for the coefficient of the linear term ($a = -0.01$). The remaining parameters were $D_i = 1$ and $b_r = 1.25$ ($c_1 = 1$, $c_2 = -0.8$). Despite the presence of non-relaxational terms in (1.1), Φ decreases monotonously (see Fig. 2) to the final value $\Phi(t = \infty) = \Phi[A = 0] = 0$ confirming its adequacy as a Lyapunov potential.

4.2. *Positive a: Benjamin–Feir stable regime*

We take in this section always $a = 1$. Non-chaotic (TW) states and spatio-temporal intermittency are the two phases found below the BF line in Fig. 1. We first perform several numerical experiments in the non-chaotic region.

A first important case is the one on the line $D_- = 0$, for which (3.11) is an exact Lyapunov functional F_{GL}. We take $D_i = -1$ and $b_r = 1$ ($c_1 = c_2 = -1$), on the $D_- = 0$ line, and compute the evolution of $\Phi = F_{GL}/L$ along a solution of (1.1), taking as initial condition for A a Gaussian noise of amplitude $\epsilon = 0.01$. Despite of the strong phase gradients present specially in the initial stages of the evolution, and of the presence of non-relaxational terms, Φ decays monotonously in time (Fig. 3). The system evolved towards a TW attractor of wave number $k = 0.0245$. The value of Φ in such state is, from Eq. (3.9), $\Phi_{k=0.0245} = -0.998796$. It is important to notice that our numerical solution for A and numerical evaluation of the derivatives in Φ reproduce this value within a 0.3% in the last time showed in Fig. 3, and continues to approach the theoretical value for the asymptotic attractor at longer times.[4]

We continue testing the Lyapunov functional for $D_i = 1$, $b_r = 1.25$ ($c_1 = 1$, $c_2 = -0.8$). This is still in the non-chaotic region but, since $D_- \neq 0$, Φ is not expected to be exact, but only a small gradient approximation. We check now the relaxation back to a stable state after a small perturbation. As initial condition we slightly perturb a TW of Eckhaus-stable wave number ($k = 0.13 < k_E$) by adding random noise of amplitude $\epsilon = 0.09$. Φ decays monotonously (Fig. 4) from its perturbed value to the value $\Phi_{k=0.13} = -0.796632$ as the perturbation is being washed out, as expected for a good Lyapunov functional.

A more demanding situation was investigated for $D_i = -1$ and $b_r = 0.5$ (again in the non-chaotic region, $c_1 = -1$ and $c_2 = -2$, and $D_- \neq 0$). Two TW of different wave numbers ($k_1 = 0.4$, $k_2 = 0.08$, both Eckhaus-stable) were joined (at two points because of the periodic boundary conditions) and the resulting state (see inset in Fig. 5) was used as initial condition. The interfaces between the two TW's contain initially discontinuities in the gradient of the phase which are washed out in a few integration steps. The two interfaces move at constant velocity but one of them remains sharp, whereas the other widens in time, progressively replacing the two initial waves. An important observation is that during the whole process the modulus of $A(x, t)$ never vanishes and then the winding number, defined as

$$\nu \equiv \int_0^L \nabla\varphi \, dx, \tag{4.1}$$

remains constant ($\nu = 20$) (with periodic boundary conditions ν is constant except at the instants in which the phase becomes singular, that is when $r = 0$). The state (limit cycle) finally reached is a TW of $k = 2\pi\nu/L = 0.245$. Despite of the complicated and non-relaxational processes occurring Φ behaves as a good Lyapunov functional monotonously decreasing from the value $\Phi(t = 0) = -1.825$ corresponding to the two-wave configuration to the value $\Phi = -1.863$ of the final attractor (Fig. 5). The dynamics of the moving fronts is more complicated than in some relaxational models [35]. For this particular set of parameters and initial wave numbers, the center of the diffuse front moves invading the region of longest wave number, while the sharp one moves towards the small wave number region.

The good behavior of Φ will be obviously lost if the field $A(x, t)$ vanishes somewhere during the evolution. As the next numerical experiment (for $D_i = 1$ and $b_r = 1.25$, that is $c_1 = 1$, $c_2 = -0.8$) we used

[4] If a smaller time step is used greater accuracy is obtained. For example, if the time step is reduced to 0.05 the value of Φ is reproduced within 10^{-7}%. But this takes quite a long computing time.

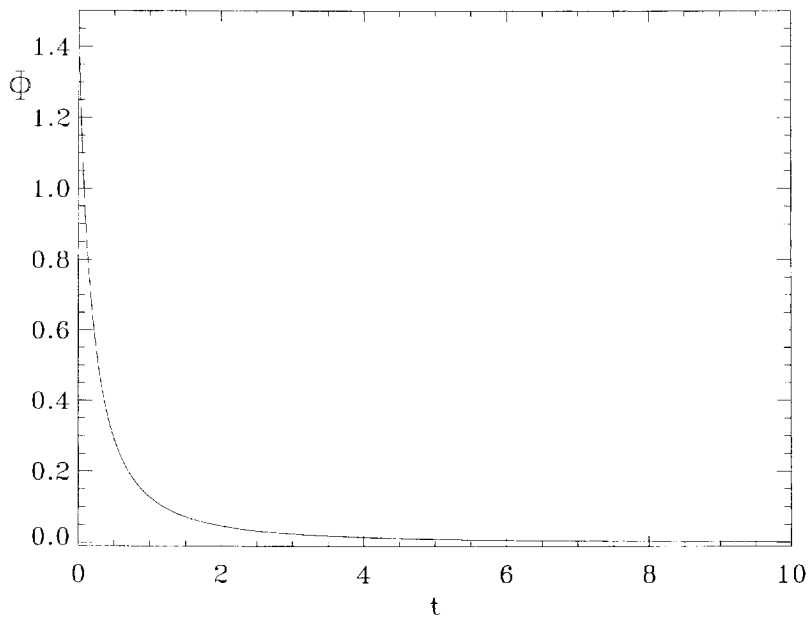

Fig. 2. Relaxation to the simple attractor for $a < 0$. The parameter values are $a = -0.01, c_1 = 1$ and $c_2 = -0.8$. The initial condition is a TW of arbitrary wave number $k = 0.295$ and arbitrary amplitude $A_0 = 1.0$.

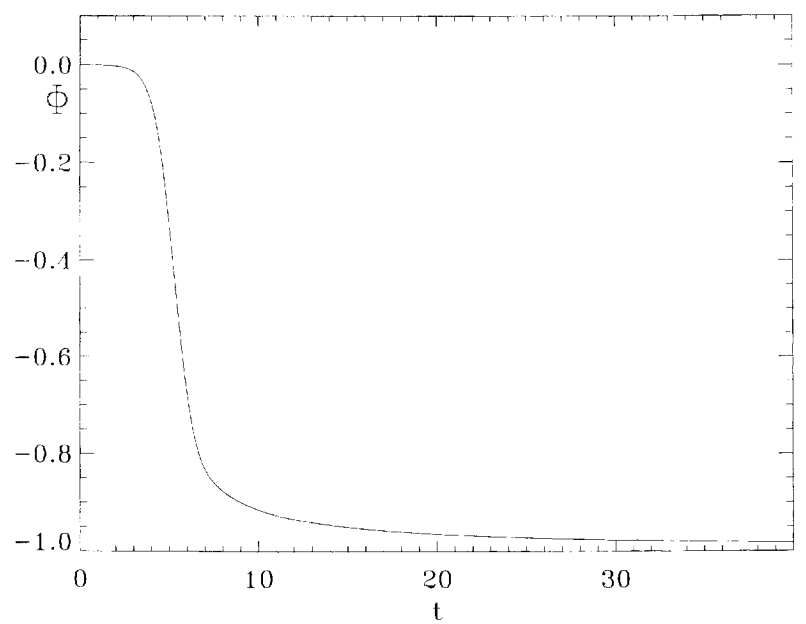

Fig. 3. Time evolution of Φ on the D_- line. The parameter values are $a = 1, c_1 = -1$ and $c_2 = -1$. The initial condition is a Gaussian noise of amplitude $\epsilon = 0.01$. The system evolved towards a TW attractor of wave number $k = 0.0245$.

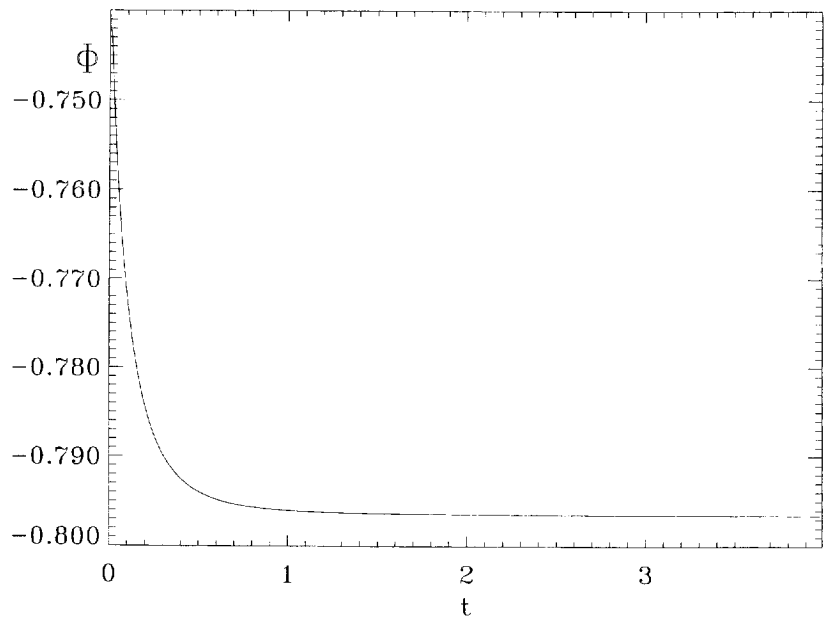

Fig. 4. Time evolution of Φ in the non-chaotic region for $c_1 = -1$ and $c_2 = -0.8$. The initial condition is an Eckhaus stable TW of wave number $k = 0.13$ perturbed by random noise of small amplitude $\epsilon = 0.09$.

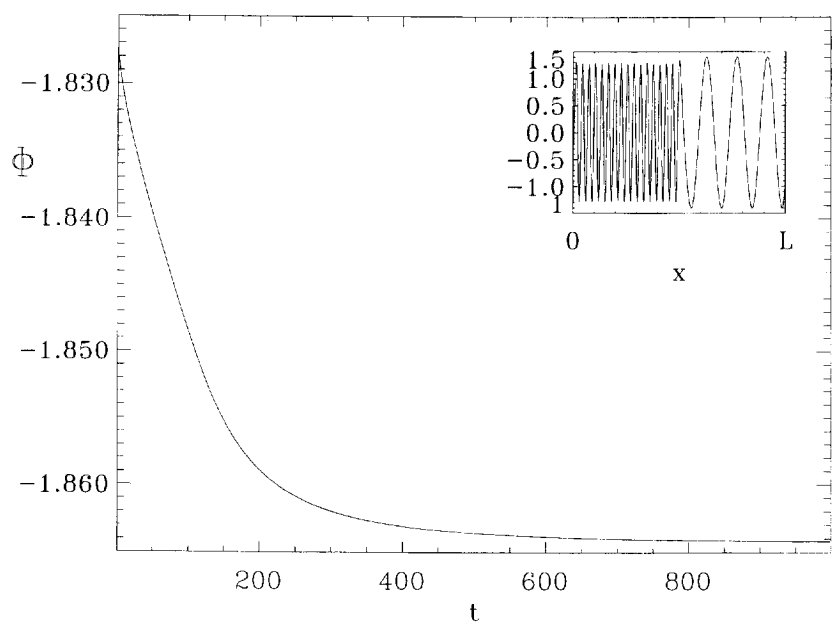

Fig. 5. Same as Fig. 4 but for $c_1 = -1$ and $c_2 = -2$. The initial condition for A consists of two Eckhaus stable TW of different wave numbers ($k_1 = 0.4, k_2 = 0.08$) joined together. The inset shows the real part of this initial configuration.

as initial condition a small ($\epsilon = 0.01$) random Gaussian noise. The system was left to evolve towards its asymptotic state (a TW). Fig. 6 shows that after a transient Φ monotonously decreases. During the initial transient it widely fluctuates, increasing and decreasing and loosing then its validity as a Lyapunov functional. This incorrect behavior occurs because during the initial stages $A(x,t)$ is small and often vanishes, changing ν. When A (and then r) vanishes the phase and (3.7) are ill-defined and out of the range of validity of a small gradient approximation. Note the contrast with the case $D_- = 0$ in which the potential is exact and well behaved even when ν is strongly changing. The particular values of the maxima and minima during the transient in which ν is changing depend on the spatial and temporal discretization, since it is clear from (3.7) that Φ is ill-defined or divergent when r vanishes. Note that this incorrect behavior of Φ for $D_- \neq 0$ is not a problem for the existence of a Lyapunov functional, but comes rather from the limited validity of the hypothesis used for its approximate construction. Nevertheless, as soon as the strong gradients disappear Φ relaxes monotonously to the value $\Phi = -0.79997$, corresponding to the final state, a TW of wave number $k = -0.0123$.

As another test in the non-chaotic region, for $D_i = -1$ and $b_r = 0.5$ ($c_1 = -1, c_2 = -2$) we use as initial condition an Eckhaus-unstable TW ($k = 0.54 > k_E = 0.48$) slightly perturbed by noise. The system evolves to an Eckhaus-stable TW ($k = 0.31$) by decreasing its winding number (initially $\nu = 44$ and finally $\nu = 26$). Fig. 7 shows the evolution of Φ from its initial value $\Phi(0) = -1.485$ the final one $\Phi = -1.77$. Although there is a monotonously decreasing baseline, sharp peaks are observed corresponding to the vanishing of r associated with the changes in ν. When ν finally stops changing, so that A is close enough to the final TW, Φ relaxes monotonously as in Fig. 4.

It was explained in Section 3 that there are parameter ranges in which Φ is smaller near the boundaries for existence of TW, that is near $k = \pm\sqrt{a/b_r}$, than for the homogeneous TW: $k = 0$. This happens for example for $D_i = 1$, $b_r = 1.25$ ($c_1 = 1, c_2 = -0.8$). The corresponding function Φ_k is shown in Fig. 8. If this prediction is true, and if Φ is a correct Lyapunov functional, evolution starting with one of these extreme and Eckhaus-unstable TW would not lead to any final TW, since this would increase the value of the Lyapunov functional. This would imply the existence for this value of the parameters of an attractor different from the TW's perhaps related to the spatio-temporal intermittency phenomenon. We use as initial condition at the parameter values of Fig. 8 an unstable TW of wave number $k = 0.64$ ($\Phi \approx -0.81$), slightly perturbed by noise. From Fig. 8, the system should evolve to a state with a value of Φ value even lower than that. What really happens can be seen in Fig. 9. The system changes its winding number from the initial value $\nu = 52$, a process during which Φ widely fluctuates and is not a correct Lyapunov functional, and ends-up in a state of $\nu = 5$, with a value of Φ larger than the initial one. After this the system relaxes to the associated stable TW of $k = 2\pi\nu/L = 0.061 < k_E = 0.23$. As clearly stated by Graham and coworkers, the expressions for the potential are only valid for small gradients. Since k is a phase gradient, results such as Fig. 8 can only be trusted for k small enough.

Finally, we show the behavior of Φ in the spatio-temporal intermittency regime. Since ν is constantly changing in this regime it is clear that (3.7) will not be a good Lyapunov functional and this simulation is included only for completeness. We take $D_i = 0$ and $b_r = 0.5$ ($c_1 = 0, c_2 = -2$) and choose as initial condition a TW with $k = 0.44 > k_E = 0.30$ ($\Phi = -1.89814$), with a small amount of noise added. The TW decreases its winding number and the system reaches soon the disordered regime called spatio-temporal intermittency. Fig. 10 shows that the time evolution of Φ is plagued with divergences, reflecting the fact that ν is constantly changing (see inset). It is interesting to observe, however, that during the initial escape from the unstable TW Φ shows a decreasing tendency, and that its average value in the chaotic regime, excluding the divergences, seems smaller than the initial one.

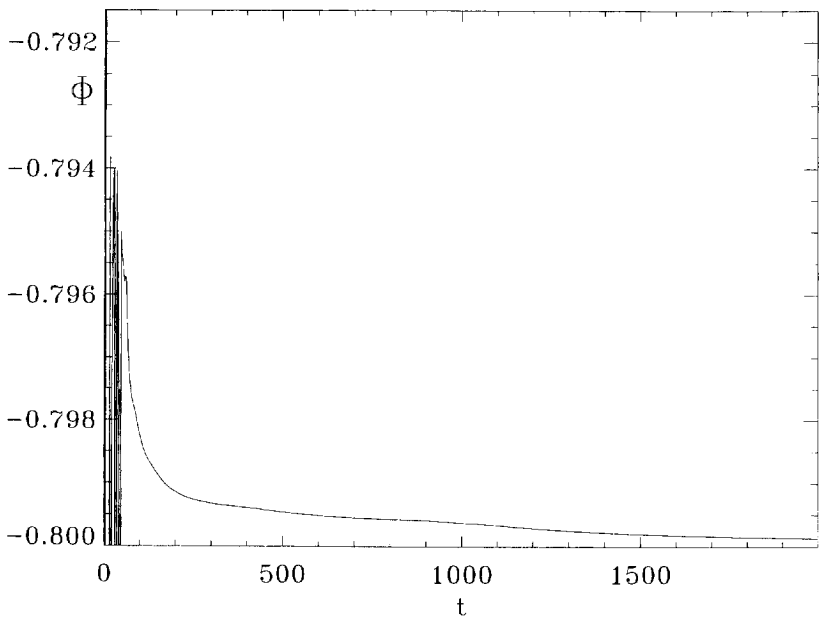

Fig. 6. Same as Fig. 4 but for $c_1 = 1$ and $c_2 = -0.8$. The initial condition is a random noise of amplitude $\epsilon = 0.01$.

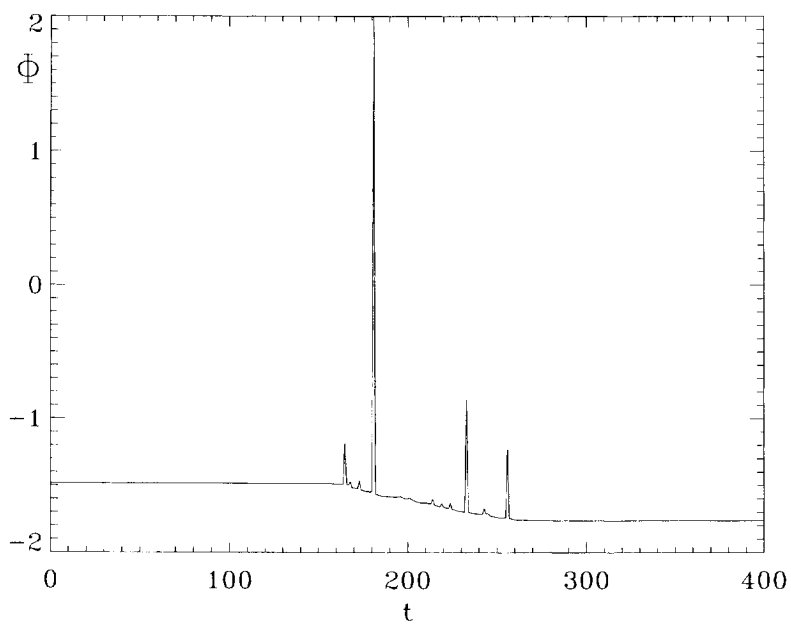

Fig. 7. Same as Fig. 4 but for $c_1 = -1$ and $c_2 = -2$. The initial condition is an Eckhaus-unstable TW ($k = 0.54 > k_E = 0.48$) slightly perturbed by noise.

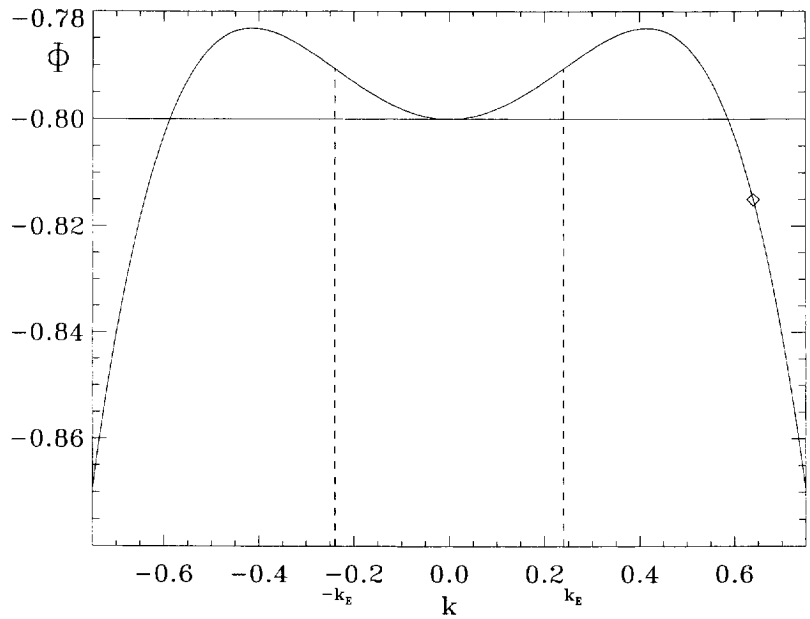

Fig. 8. The function $\Phi_k \equiv \Phi[A_k]$ as a function of k. The parameter values are $a = 1, c_1 = 1$ and $c_2 = -0.8$. The values of k_E are indicated by dashed lines. The diamond indicates the point $\Phi_{k=0.64}$ taken as initial condition for the simulation in Fig. 9.

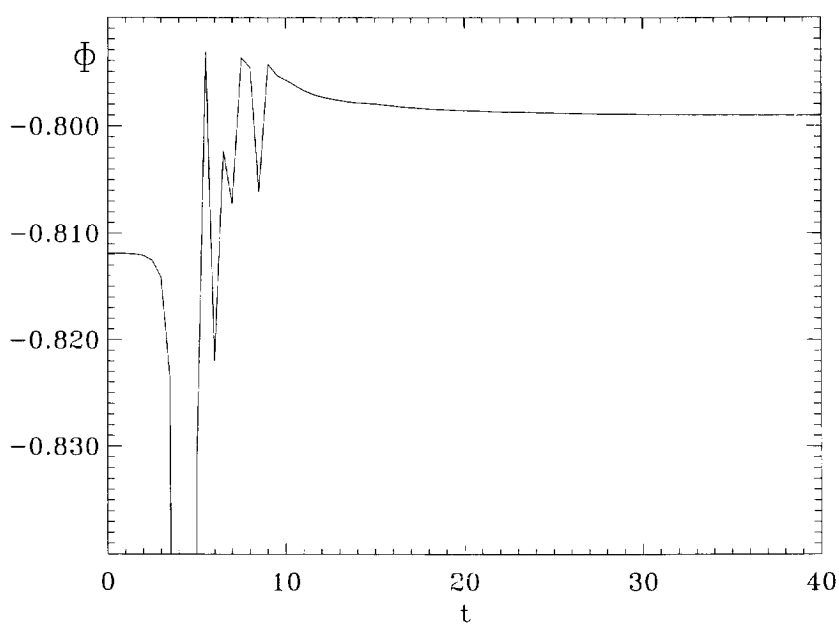

Fig. 9. Time evolution of Φ for $c_1 = 1$ and $c_2 = -0.8$. The initial condition is an Eckhaus-unstable TW ($k = 0.64 > k_E = 0.48$) slightly perturbed by noise.

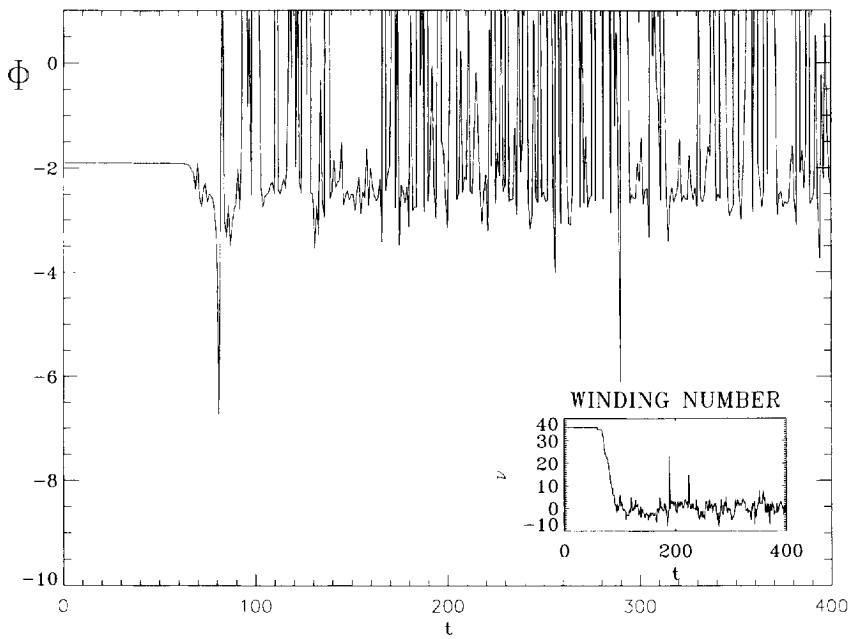

Fig. 10. Time evolution of Φ in the STI region ($c_1 = 0.0$ and $c_2 = -2$). The initial condition is an Eckhaus-unstable TW ($k = 0.45 > k_E = 0.30$) slightly perturbed by noise. The winding number evolution is plotted in the inset.

5. Numerical studies of the Lyapunov functional in the phase turbulence regime

The phase turbulence regime is characterized by the absence of phase singularities (thus ν is constant). This distinguishes it as the only chaotic regime for which Φ would be well defined. Graham and co-workers [14,30] derived especially for this region an expression proposed as Lyapunov functional in the small gradient approximation (3.12).

We recall that the calculations in [14,30] predict that the phase turbulent attractor lies on a potential plateau, consisting of all the complex functions satisfying (3.14), in which all the unstable TW cycles are also embedded. The value of the potential on such plateau can be easily calculated by substituting in (3.12) an arbitrary TW, and the result is

$$\Phi_{\mathrm{pl}} = -\frac{a^2}{b_r}. \tag{5.1}$$

We note that this value does not depend on D_i or D_r and then it is independent of c_1, the vertical position in the diagram of Fig. 1, within the phase turbulence region.

In this section we take also $a = 1$. We perform different simulations for $D_i = 1.75$ and $b_r = 1.25$ ($c_1 = 1.75$, $c_2 = -0.8$). In the first one, we start the evolution with the homogeneous oscillation solution (TW of $k = 0$). This solution is linearly unstable, but since no perturbation is added, the system does not escape from it. The potential value predicted by (5.1) is $\Phi_{\mathrm{pl}} = -0.8$. This value is reproduced by the numerical simulation up to the sixth significant figure for all times (Fig. 11, solid line). This agreement, and the fact that the unstable TW is maintained, gives confidence in our numerical procedure.

In a second simulation, a smooth perturbation (of the form μe^{iqx} with $q = 0.049$ and $\mu = 0.09$) is added to the unstable TW and the result used as initial condition. This choice of perturbation was taken to remain as much as possible within the range of validity of the small gradient hypothesis. After a transient the perturbation grows and the TW is replaced by the phase turbulence state (the winding number remains fixed to 0). The corresponding evolution of Φ

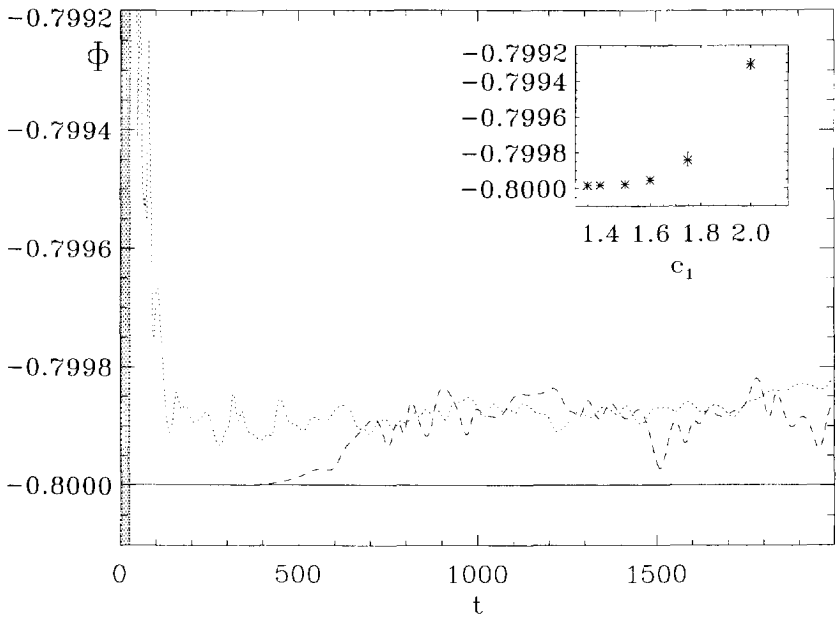

Fig. 11. Time evolution of Φ in the phase turbulence region ($c_1 = 1.75$ and $c_2 = -0.8$). Solid line: evolution of an unperturbed unstable traveling wave. Dotted line: evolution from noise. Dashed line: evolution from a slightly perturbed traveling wave. The inset shows final average values of Φ as a function of the c_1 parameter ($c_2 = -0.8$). The error bars indicate the standard deviation of the fluctuations around the average value.

is shown in Fig. 11 (long-dashed line). The value of the potential increases from $\Phi_{\rm pl}$ to a higher value, and then irregularly oscillates around it. Both the departure and the fluctuation are very small, of the order of 10^{-4} times the value of Φ. Simulations with higher precisions confirm that these small discrepancies from the theoretical predictions are not an artifact of our numerics, but should be attributed to the terms with higher gradients which are not included in (3.12). As a conclusion, the prediction that the phase turbulence dynamics, driven by non-relaxational terms, maintains constant Φ in a value equal to the one for TW is confirmed within a great accuracy.

However, it is interesting to study how systematic are the small deviations from the theory. To this end we repeat the launching of the TW with a small perturbation for several values of $D_i = c_1$, for the same value of b_r as before. The prediction is that Φ should be independent of c_1. The inset in Fig. 11 shows that the theoretical value $\Phi_{pl} = -0.8$ is attained near the BF line, and that as c_1 is increased away from the BF line there are very small but systematic discrepancies. The values shown for the potential are time averages of its instantaneous values, and the error bars denote the standard deviation of the fluctuations around the average.

Again for $c_1 = 1.75$, $c_2 = -0.8$, we perform another simulation (Fig. 11, short-dashed line) consisting in starting the system in a random Gaussian noise configuration, of amplitude 0.01, and letting it to evolve towards the phase turbulence attractor. As in other cases, there is a transient in which Φ is ill-defined since the winding number is constantly changing. After this Φ decreases. This decreasing is not monotonous but presents small fluctuations around a decreasing trend. The decreasing finally stops and Φ remains oscillating around approximately the same value as obtained from the perturbed TW initial condition. The final state has $\nu = -1$, so that in fact the attractor reached is different from the one in the previous runs ($\nu = 0$) but the difference is the smallest possible and the difference in value of the associated

potential cannot be distinguished within the fluctuations of Fig. 11. These observations confirm the idea of a potential which decreases as the system advances towards an attractor, and remains constant there, but at variance with the cases in the non-chaotic region here the decreasing is not perfectly monotonous, and the final value is only approximately constant.

Since the small discrepancies with the theory increase far from the BF line, and since it is known that condition (3.14) can be obtained from an adiabatic-following of the modulus to the phase that looses accuracy far from the BF line, one is lead to consider the role of adiabatic following on the validity of Φ as a potential. To this end we evaluated Φ along trajectories $A(x,t)$ constructed with the phase obtained from solutions of (1.1), but with modulus replaced by (3.14), so enforcing the adiabatic following of the modulus to the phase. No significant improvement was obtained with respect to the cases in which the adiabatic following was not enforced since that, in fact, adiabatic following was quite well accomplished by the solution of (1.1). Then it is not the fact that the solutions of (1.1) do not fulfill (3.14) exactly, but the absence of higher gradient terms in both (3.14) and (3.12) the responsible for the small failures in the behavior of Φ.

Finally, it is interesting to show that the Lyapunov potential Φ can be used as a diagnostic tool for detecting changes in behavior that would be difficult to monitor by observing the complete state of the system. For example the time at which the phase turbulence attractor is reached can be readily identified from the time-behavior of Φ in Fig. 11. More interestingly it can be used to detect the escape from metastable states. For example, Fig. 12 shows Φ for evolution from a Gaussian noise initial condition ($\epsilon = 0.01$). $D_i = 2$ and $b_r = 1.25$ ($c_1 = 2$, $c_2 = -0.8$). The system reaches first a long lived state with $\nu = 2$ not too different from the usual phase turbulent state of $\nu = 2$. After a long time, however, the system leaves this metastable state and approaches a more ordered state that can be described [36] as phase turbulent fluctuations around quasi-periodic configurations related to those of [28]. More details about this state will be described elsewhere [36]. What is of interest here is that from Fig. 12 one can easily identify the changes between the different dynamical regimes. In particular the decrease in the fluctuations of Φ near $t \approx 1000$ identifies the jump from the first to the second turbulence regimes.

6. Conclusions and outlook

The validity of the expressions for the Lyapunov functional of the CGLE found by Graham and coworkers has been numerically tested. The most important limitation is that they were explicitly constructed in an approximation limited to small gradients of modulus and phase. This precludes its use for evolution on attractors such that zeros of r and thus phase singularities appear (defect turbulence, bi-chaos, spatio-temporal intermittency). The same problem applies to transient states of evolution towards more regular attractors, if phase singularities appear in this transient (for instance decay of an Eckhaus unstable TW, evolution from random states close to $A = 0$, etc.). It would be interesting to have the expansion of the Lyapunov potential for small gradients of the real and imaginary components of A, instead of using polar coordinates. This would eliminate the problem of the ill-definition of the phase, and clarify further the stability of the gradient expansion.

Apart from this, if changes in winding number are avoided, expressions (3.6), (3.7), and (3.12) display the correct properties of a Lyapunov functional: minima on stable attractors, where non-relaxational dynamics maintains it in a constant value, and decreasing value during approach to the attractor. These properties are completely satisfied in the non-chaotic region of parameter space, even in complex situations such as TW competition, as long as large gradients do not appear. It is remarkable that, although the potential is constructed through an expansion around the $k = 0$ TW, its minima identify exactly the remaining TW, its stability, and the non-relaxational terms calculated by subtracting the potential terms to (1.1) give exactly their frequencies. In the phase turbulence regime, however, there are small discrepancies with respect to the theoretical predictions: lack of monotonicity in the approach to the attractor, small fluctuations around the asymptotic value, and small

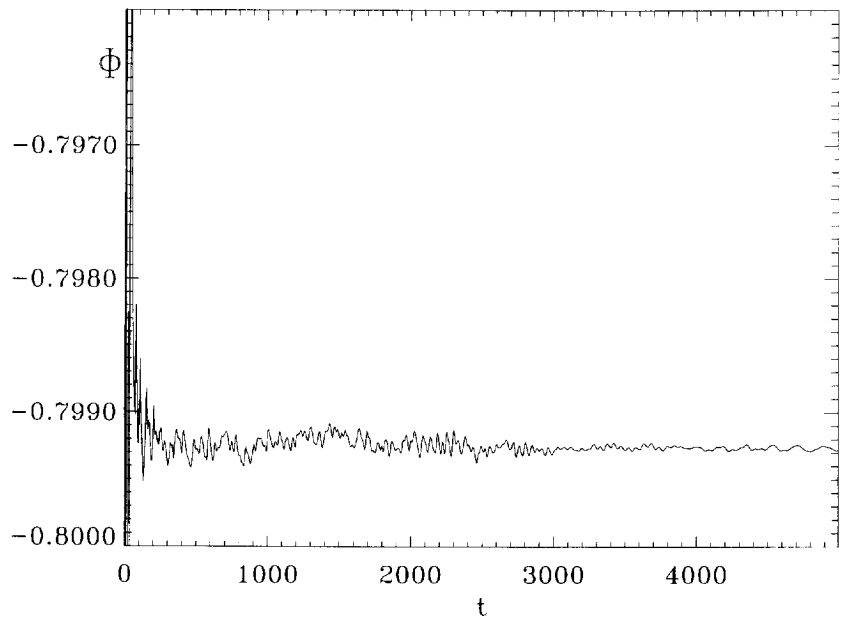

Fig. 12. Same as Fig. 11 but for $c_1 = 2$ and $c_2 = -0.8$. The initial condition was random noise with an amplitude $\epsilon = 0.01$, time step 0.005. In this case 2048 Fourier modes were taken into account. Note the transition occurring arround $t \approx 1000$ to a less fluctuating state.

discrepancy between the values of the potential of TW's and of turbulent configurations, that were predicted to be equal. All these deviations are very small but systematic, and grow as we go deeper in the phase turbulence regime. They can be fixed in principle by calculating more terms in the gradient expansion.

In addition in order to clarify the conceptual status of non-relaxational and non-potential dynamical systems one can ask about the utility of having approximate expressions for the Lyapunov functional of the CGLE. Several applications have been already developed for the case in which (1.1) is perturbed with random noise. In particular the stationary probability distribution is directly related to Φ, and in addition barriers and escape times from metastable TW have been calculated [12,30]. In the absence of random noise, Φ should be still useful in stating the nonlinear stability of the different attractors. However, in practice there will be limitations in the validity of the predictions, since Φ has been constructed in an expansion which is safe only near one particular attractor (the homogeneous TW).

Once known Φ, powerful statistical mechanics techniques (mean field, renormalization group, etc.) can in principle be applied to it to obtain information on the static properties of the CGLE (the dynamical properties, as time-correlation functions, would depend also on the non-relaxational terms N, as in critical dynamics [15]). Zero-temperature Monte Carlo methods can also be applied to sample the phase turbulent attractors, as an alternative to following the dynamical evolution on it. All those promising developments will have to face first with the complexity of Eqs. (3.6), (3.7), and (3.12). Another use of Lyapunov potentials (the one most used in equilibrium thermodynamics) is the identification of attractors by minimization instead of by solving the dynamical equations. In the case of the TW attractors, solving the Euler–Lagrange equations for the minimization of Φ is in fact more complex than solving directly the CGLE with a TW ansatz. But the limit cycle character of the attractors, and their specific form, is derived, not guessed as when substituting the TW ansatz. For the case of chaotic attractors (as in the phase turbulence regime) minimization

of potentials can provide a step towards the construction of inertial manifolds. In this respect it should be useful considering the relationships between the Lyapunov potential of Graham and coworkers and other objects based on functional norms used also to characterize chaotic attractors [37,38].

Acknowledgements

We acknowledge very helpful discussions on the subject of this paper with R. Graham. We also acknowledge helpful inputs of E. Tirapegui and R. Toral on the general ideas of non-equilibrium potentials, and from A. Amengual on the numerical code. We acknowledge financial support from DGYCIT (Spain) Projects PB94-1167 and PB94-1172. R.M. also acknowledges partial support from the Programa de Desarrollo de las Ciencias Básicas (PEDECIBA, Uruguay), the Consejo Nacional de Investigaciones Científicas Y Técnicas (CONICYT, Uruguay) and the Programa de Cooperación con Iberoamérica (ICI, Spain).

References

[1] M.C. Cross and P.C. Hohenberg, Rev. Modern Phys. 65 (1993) 851 and references therein.
[2] W. van Saarloos and P. Hohenberg, Physica D 56 (1992) 303 .
[3] P. Kolodner, Phys. Rev. E 50 (1994) 2731.
[4] P. Coullet, L. Gil and F. Roca, Optimal Comm. 73 (1989) 403.
[5] Y. Kuramoto and S. Koga, Progr. Theor. Phys. Suppl. 66 (1981) 1081 .
[6] B.I. Shraiman, A. Pumir, W. van Saarloos, P.C. Hohenberg, H. Chaté and M. Holen, Physica D 57 (1992) 241.
[7] H. Chaté, Nonlinearity 7 (1994) 185.
[8] H. Chaté, Spatiotemporal Pattern in Nonequilibrium Complex Systems (Addison–Wesley, New York, 1994), Santa Fe Institute in the Sciences of Complexity.
[9] H. Chate, New Trends in Nonlinear Dynamics: Nonvariational Aspects (North-Holland, Estella, Spain, 1991), appeared in Physica D 61.
[10] R. Graham and T. Tél, Europhys. Lett. 13 (1990) 1715.
[11] R. Graham and T. Tél, Phys. Rev. A 42 (1990) 4661.
[12] R. Graham and T. Tél, in: Instabilities and Nonequilibrium Structures III, eds. E. Tirapegui and W. Zeller (Reidel, Dordrecht, 1991) p. 125.
[13] O. Descalzi and R. Graham, Phys. Lett. A 170 (1992) 84.
[14] O. Descalzi and R. Graham, Z. Phys. B 93 (1994) 509.
[15] P. C. Hohenberg and B.I. Halperin, Rev. Mod. Phys. 49 (1978) 535.
[16] J.D. Gunton, M. San Miguel and P. Sahni, in: Phase Transitions and Critical Phenomena eds. C. Domb and J. L. Lebowitz (Academic Press, London, 1983) Vol. 8.
[17] R. Graham, in: Theory of continuous Fokker–Plank systems, Vol. 1 of Noise in nonlinear dynamical systems, eds. F. Moss and P.V.E.M. Clintock (Cambridge University Press, Cambridge, 1989) p.225.
[18] R. Graham, in: XXV Years of Nonequilibrium Statistical Mechanics, Vol. 446 of Lecture Notes in Mathematics, eds. L. Brey, J. Marro, M. Rubí and M. San Miguel (Springer, Berlin, 1995).
[19] M. Caponeri and S. Ciliberto, Phys. Rev. Lett. 64 (1990) 2775.
[20] M. Caponeri and S. Ciliberto, Physica D 58 (1992) 365.
[21] H. Calisto, E. Cerdá and E. Tirapegui, J. Statist. Phys. 69 (1992) 1115.
[22] M. San Miguel and F. Sagués, Phys. Rev. A 36 (1987) 1883.
[23] P. Szépfalusy and T. Tél, Phys. Rev. A 112 (1982) 146.
[24] S. Rica and E. Tirapegui, Phys. Rev. Lett. 64 (1990) 878.
[25] T.B.Benjamin and J.E. Feir, J. Fluid Mech. 27 (1967) 417.
[26] A. Newell, Appl. Math. 15 (1974) 157.
[27] W. Eckhaus, Studies in Nonlinear Stability Theory (Springer, Berlin, 1965).
[28] B. Janiaud, A. Pumir, D. Bensimon, V. Croquette, H. Richter and L. Kramer, Physica D 55 (1992) 269.
[29] D. Egolf and H. Greenside, Phys. Rev. Lett. 74 (1995) 1751.
[30] O. Descalzi, Ph.D. Thesis, University of Essen (1993).
[31] R. Graham, in: Fluctuations, Instabilities and Phase Transitions, ed. T. Riste (Plenum Press, New York, 1975) p.270.
[32] D. Walgraef, G. Dewl and P. Borkmans, Adv. Chem. Phys. 49 (1982) 311.
[33] D. Walgraef, G. Dewl and P. Borkmans, J. Chem. Phys. 78 (1983) 3043.
[34] H. Sakaguchi, Progr. Theor. Phys. 84 (1990) 792.
[35] S. Chan, J. Chem. Phys. 67 (1977) 5755.
[36] R. Montagne, E. Hernández-García and M. San Miguel, to be published.
[37] C.R. Doering, J.D. Gibbon, D.D. Holm and B. Nicolaenko, Nonlinearity 1 (1988) 279.
[38] M. Bartuccelli, P. Constantin, C.R. Doering, J.D. Gibbon and M. Gisselfält, Physica D 44 (1990) 421.